Inorg. Chem. **2006**, *45*, 8492–8499

Ultrahigh-Field NMR Spectroscopy of Quadrupolar Transition Metals: ^{55}Mn NMR of Several Solid Manganese Carbonyls

Kristopher J. Ooms,[†] Kirk W. Feindel,[†] Victor V. Terskikh,[‡] and Roderick E. Wasylishen*[,†]

Department of Chemistry, University of Alberta, Edmonton, Alberta T6G 2G2, Canada, and Department of Chemistry, University of Ottawa, Ottawa, Ontario K1N 6N5, Canada

Received May 16, 2006

^{55}Mn NMR spectra acquired at 21.14 T ($\nu_L(^{55}Mn) = 223.1$ MHz) are presented and demonstrate the advantages of using ultrahigh magnetic fields for characterizing the chemical shift tensors of several manganese carbonyls: η^5-CpMn(CO)$_3$, Mn$_2$(CO)$_{10}$, and (CO)$_5$Mn*M*Ph$_3$ (*M* = Ge, Sn, Pb). For the compounds investigated, the anisotropies of the manganese chemical shift tensors are less than 250 ppm except for η^5-CpMn(CO)$_3$, which has an anisotropy of 920 ppm. At 21.14 T, one can excite the entire $m_I = 1/2 \leftrightarrow m_I = -1/2$ central transition of η^5-CpMn(CO)$_3$, which has a breadth of approximately 700 kHz. The breadth arises from second-order quadrupolar broadening due to the ^{55}Mn quadrupolar coupling constant of 64.3 MHz, as well as the anisotropic shielding. Subtle variations in the electric field gradient tensors at the manganese are observed for crystallographically unique sites in two of the solid pentacarbonyls, resulting in measurably different C_Q values. MQMAS experiments are able to distinguish four magnetically unique Mn sites in (CO)$_5$MnPbPh$_3$, each with slightly different values of δ_{iso}, C_Q, and η_Q.

Introduction

The latest developments in ultrahigh-field NMR magnets have resulted in an increased ability to probe the environments of many transition metal nuclei via solid-state NMR, SSNMR.[1−6] Most NMR-active transition metal nuclei are quadrupolar with noninteger spin and typically yield broad NMR powder patterns in the solid state. Due to the inverse magnetic field dependence of the second-order quadrupolar interaction, broadening of the $m_I = 1/2 \leftrightarrow m_I = -1/2$ central transition can be reduced by performing experiments at the highest applied magnetic fields available. With the advent of commercially available magnets operating at 21.1 T, the possibility of studying a wide range of inorganic and organometallic compounds using transition metal NMR is increasing.[7]

Manganese NMR spectroscopy has been limited due to the relatively large quadrupole moment of ^{55}Mn, $Q = 33$ fm^2,[8] which can result in large ^{55}Mn quadrupolar couplings. ^{55}Mn nuclear quadrupolar coupling constants, C_Q, have been measured ranging from 1.58 MHz for $KMnO_4$ to 85.8 MHz for Ni(1,10-phen)$_3$[(Ph$_3$P)$_2$Mn(CO)$_4$]$_2$.[9,10] The larger C_Q values are typically determined by nuclear quadrupole resonance, NQR, and Mössbauer spectroscopic investigations of solid samples or by microwave spectroscopy of molecules in the gas phase. ^{55}Mn has a spin $I = 5/2$, a natural abundance of 100%, a Larmor frequency close to that of ^{13}C,[11] and a chemical shift range of approximately 3500 ppm. A survey of the ^{55}Mn NMR literature indicates that the manganese of Mn(CO)$_3$(MeCN)$_3^+$ is the least shielded, $\delta_{iso} = 490$ ppm, while the manganese of MnH(PF$_3$)$_5$ is the most shielded, $\delta_{iso} = -2953$ ppm, relative to $MnO_4^-{}_{(aq)}$.[12,13] Early reviews

* To whom correspondence should be addressed. E-mail: roderick.wasylishen@ualberta.ca. Tel: (780) 492-4336. Fax: (780) 492-8231.
[†] University of Alberta.
[‡] University of Ottawa.

(1) Ooms, K. J.; Wasylishen, R. E. *J. Am. Chem. Soc.* **2004**, *126*, 10972−10980.
(2) Bryce, D. L.; Wasylishen, R. E. *Phys. Chem. Chem. Phys.* **2002**, *4*, 3591−3600.
(3) Bryce, D. L.; Wasylishen, R. E. *Phys. Chem. Chem. Phys.* **2001**, *3*, 5154−5157.
(4) Lipton, A. S.; Heck, R. W.; Ellis, P. D. *J. Am. Chem. Soc.* **2004**, *126*, 4735−4739.
(5) De Lacaillerie, J. B. D.; Barberon, F.; Romanenko, K. V.; Lapina, O. B.; Le Polles, L.; Gautier, R.; Gan, Z. H. *J. Phys. Chem. B* **2005**, *109*, 14033−14042.
(6) Larsen, F. H.; Farnan, I.; Lipton, A. S. *J. Magn. Reson.* **2006**, *178*, 228−236.
(7) *Can. Chem. News* **2006**, *April*, 5.
(8) Pyykkö, P. *Mol. Phys.* **2001**, *99*, 1617−1629.
(9) Wadsworth, M.; France, P. W. *J. Magn. Reson.* **1983**, *51*, 424−429.
(10) Pribula, C. D.; Brown, T. L.; Münck, E. *J. Am. Chem. Soc.* **1974**, *96*, 4149−4154.
(11) Harris, R. K.; Becker, E. D.; De Menezes, S. M. C.; Goodfellow, R.; Granger, P. *Pure Appl. Chem.* **2001**, *73*, 1795−1818.
(12) Rehder, D.; Bechthold, H.-Ch.; Keçeci, A.; Schmidt, H.; Siewing, M. *Z. Naturforsch.* **1982**, *37b*, 631−645.

10.1021/ic0608445 CCC: $33.50
Published on Web 07/27/2006

of the ^{55}Mn NMR literature have been presented by Kidd and Goodfellow,[14] as well as Rehder;[15] more recent reviews have been published by Granger[16] and Pregosin.[17] There have been only a few ^{55}Mn NMR studies of compounds in the solid state, most of them performed on powders of permanganate salts or single crystals.[9,18−24] Particularly significant are the early ^{55}Mn single-crystal NMR investigations of Sheline and co-workers,[23,24] which provided evidence that the anisotropy of the manganese shielding could be as large as 1000 ppm.

Manganese chemistry is a growing area of research, owing to the use of Mn in organic and inorganic synthesis;[25] manganese is a relatively inexpensive transition metal that can be used for a variety of oxidation, substitution, and catalytic reactions.[25] Additionally, methylcyclopentadieneyl manganese tricarbonyl, $MeCpMn(CO)_3$, is finding increased use as an anti-knock fuel additive throughout North America.[26] The bonding environment about manganese in organomanganese compounds often dictates their reactivity. Since SSNMR is an ideal technique for probing the subtle variations in the electronic−molecular structure about a nucleus, the ability to perform SSNMR of ^{55}Mn compounds cannot be overemphasized.

In the present study, we demonstrate the advantages of acquiring ^{55}Mn NMR spectra at 21.14 T and illustrate some of the valuable information that can be obtained at this field strength. We have obtained ^{55}Mn NMR spectra of five solid diamagnetic compounds, η^5-$CpMn(CO)_3$, $Mn_2(CO)_{10}$, and $(CO)_5MnMPh_3$ (M = Ge, Sn, Pb) and have fully characterized both their ^{55}Mn EFG and chemical shift tensors. The possibility of resolving crystallographically nonequivalent Mn sites has also been illustrated for two of the compounds.

Experimental Section

η^5-$CpMn(CO)_3$ and $Mn_2(CO)_{10}$ were purchased from Aldrich and used without further purification. The $(CO)_5MnMPh_3$ (M = Ge, Sn, Pb) compounds were prepared under nitrogen by reacting $NaMn(CO)_5$ with the appropriate $ClMPh_3$ and subsequently recrystalized from hexane in the air.[27,28]

^{55}Mn NMR experiments were performed on Bruker Avance spectrometers at 7.05 (74.5 MHz), 11.75 (124.0 MHz), and 21.14 T (223.1 MHz). The experiments at 21.14 T were performed at the National Ultrahigh-field NMR Facility for Solids in Ottawa, Canada; experiments at 11.75 and 7.05 T were performed at the University of Alberta. Bruker double- and triple-resonance magic angle spinning, MAS, probes (4, 3.2, and 2.5 mm o.d.) were used. All ^{55}Mn NMR chemical shifts were referenced with respect to a 0.82 m aqueous solution of $KMnO_4$, $\delta = (\nu_{sample} - \nu_{ref})/\nu_{ref}$.[11] The ^{55}Mn $\pi/2$ pulse lengths were determined for the setup sample, 0.82 m $KMnO_4$, and ranged from 1.6 to 2.5 μs depending on the spectrometer used. An echo ($\pi/2 - \tau_1 - \pi/2 - \tau_2 -$ ACQ or $\pi/2 - \tau_1 - \pi - \tau_2 -$ ACQ) pulse sequence was used for acquiring ^{55}Mn NMR spectra with pulse lengths, $\tau_{p(sel)}$, that selectively excited the central transition, $\tau_{p(sel)} = \tau_{p(non-sel)}/(I + 1/2) = \tau_{p(non-sel)}/3$; in some cases, the pulse widths were optimized on the samples to reduce line shape distortions.[29] The quadrupolar Carr-Purcell Meiboom-Gill, QCPMG,[30,31] experiment was used to acquire stepped-frequency spectra which were co-added using the sky-line projection method.[32] A 3-pulse sequence with z-filter was used to acquire 3Q MAS spectra of $(CO)_5MnPbPh_3$; $p1 - t_{1(3Q)} - p2 - t_{(ZQF)} - p3 -$ ACQ.[33] Excitation ($p1 = 1.95$ μs) and conversion ($p2 = 0.65$ μs) pulses were applied with an RF field amplitude of 130 kHz; the weak central-transition selective pulse was $p3 = 17$ μs, corresponding to an RF field of 5 kHz. The sample spinning speed was 15 kHz using a 2.5 mm Bruker MAS probe. The acquisition matrix was $2048(t_2) \times 128(t_1)$ with 192 scans accumulated for each t_1. Shearing transformation was performed during data processing. The 1D spectra used for line shape analysis were extracted from the 2D spectrum and simulated with WSolids, a program developed in the Wasylishen laboratory.

EFG[34] and magnetic shielding calculations of η^5-$CpMn(CO)_3$ were performed with the relativistic ZORA-DFT formalism in the Amsterdam Density Functional (ADF 2004.01) package.[35−41] The ZORA valence triple-ζ doubly polarized, TZ2P, basis set was used for all nuclei. The local density approximation of VWN[42] and generalized gradient approximation of Becke88[43] and Perdew86[44,45]

(13) Miles, W. J.; Garrett, B. B.; Clark, R. J. *Inorg. Chem.* **1969**, *8*, 2817−2818.
(14) Kidd, R. G.; Goodfellow, R. J. In *NMR and the Periodic Table*; Harris, R. K., Mann, B. E., Eds.; Academic Press: London, 1979; pp 218−222.
(15) Rehder, D. In *Multinuclear NMR*; Mason, J., Ed.; Plenum: New York, 1989; pp 507−511.
(16) Granger, P. In *Encyclopedia of NMR*; Grant, D. M., Harris, R. K., Eds.; John Wiley and Sons: Chichester, 2002; Vol. 6, pp 3889−3900.
(17) Pregosin, P. S. *Transition Metal Nuclear Magnetic Resonance*; Elsevier: Amsterdam, 1991.
(18) Segel, S. L. *J. Chem. Phys.* **1969**, *51*, 848−850.
(19) Mooberry, E. S.; Sheline, R. K. *J. Chem. Phys.* **1972**, *56*, 1852−1855.
(20) Mooberry, E. S.; Spiess, H. W.; Sheline, R. K. *J. Chem. Phys.* **1972**, *57*, 813−821.
(21) Burton, D. J.; Harris, R. K. *Chem. Commun.* **1982**, 256−257.
(22) Tarasov, V. P.; Kirkakosyan, G. A.; Meladze, M. A.; German, K. É. *Koordinats. Khim.* **1993**, *19*, 269−283.
(23) Spiess, H. W.; Sheline, R. K. *J. Chem. Phys.* **1971**, *54*, 1099−1103.
(24) Slater, J. L.; Pupp, M.; Sheline, R. K. *J. Chem. Phys.* **1972**, *57*, 2105−2108.
(25) Sweigart, D. A.; Reingold, J. A. In *Encyclopedia of Inorganic Chemistry*; King, R. B., Ed.; Wiley: Chichester, 2005; Vol. 5, p 2907.
(26) *Toxicological Profile for Manganese*; U.S. Department of Health and Human Services: Washington, DC, 2000; p 329.
(27) Gorsich, R. D. *J. Am. Chem. Soc.* **1962**, *84*, 2486−2491.
(28) $NaMn(CO)_5$ was prepared by addition of $Mn_2(CO)_{10}$ to a Na amalgam (0.5 g Na in 3 mL Hg) in dry THF. The $NaMn(CO)_5$ solution was then transferred to a flask containing the appropriate $ClMPh_3$ and allowed to react for 2 h. The solvent was reduced to half volume, poured into cold water, and filtered, and then the precipitate was extracted with hot hexane (yields 70−80%).
(29) Bodart, P. R.; Amoureux, J.-P.; Dumazy, Y.; Lefort, R. *Mol. Phys.* **2000**, *98*, 1545−1551.
(30) Larsen, F. H.; Jakobsen, H. J.; Ellis, P. D.; Nielsen, N. C. *J. Magn. Reson.* **1998**, *131*, 144−147.
(31) Larsen, F. H.; Jakobsen, H. J.; Ellis, P. D.; Nielsen, N. C. *J. Phys. Chem. A* **1997**, *101*, 8597−8606.
(32) Lipton, A. S.; Wright, T. A.; Bowman, M. K.; Reger, D. L.; Ellis, P. D. *J. Am. Chem. Soc.* **2002**, *124*, 5850−5860.
(33) Amoureux, J.-P.; Fernandez, C.; Steuernagel, S. *J. Magn. Reson. A* **1996**, *123*, 116−118.
(34) van Lenthe E.; Jan Baerends, E. *J. Chem. Phys.* **2000**, *112*, 8279−8291.
(35) Schreckenbach, G.; Ziegler, T. *J. Phys. Chem.* **1995**, *99*, 606−611.
(36) Schreckenbach, G.; Ziegler, T. *Int. J. Quantum Chem.* **1996**, *60*, 753−766.
(37) Schreckenbach, G.; Ziegler, T. *Int. J. Quantum Chem.* **1997**, *61*, 899−918.
(38) Wolff, S. K.; Ziegler, T. *J. Chem. Phys.* **1998**, *109*, 895−905.
(39) Wolff, S. K.; Ziegler, T.; van Lenthe, E.; Baerends, E. J. *J. Chem. Phys.* **1999**, *110* 7689−7698.
(40) Guerra, C. F.; Snijders, J. G.; te Velde, G.; Baerends, E. J. *Theor. Chem. Acc.* **1998**, *99*, 391−403.
(41) *ADF 2004.01, SCM [online], Theoretical Chemistry*; Vrije Universiteit: Amsterdam, Availaible from http://www.scm.com.
(42) Vosko, S. H.; Wilk, L.; Nusair, M.; *Can. J. Phys.* **1980**, *58*, 1200−1211.
(43) Becke, A. D. *Phys. Rev. A* **1988,** *38*, 3098−3100.

Table 1. Solid-State ^{55}Mn NMR Parameters for the Five Compounds Studied[a]

	C_Q/MHz	η_Q	δ_{iso}/ppm	Ω/ppm	κ	α/°	β/°	γ/°
η^5-CpMn(CO)$_3$	64.3 ± 0.5	0.02 ± 0.02	−2200 ± 10	920 ± 10	0.95 ± 0.05	0 ± 10	0 ± 10	0 ± 10
calculated	66.3	0.01	−2155	567	0.80	0	0	0
Mn$_2$(CO)$_{10}$	3.28 ± 0.05	0.35 ± 0.02	−2288 ± 2	105 ± 10	0.95 ± 0.05	90 ± 10	90 ± 5	0 ± 10
(CO)$_5$MnGePh$_3$	24.6 ± 0.2	0.36 ± 0.05	−2468 ± 3	220 ± 20	−0.9 ± 0.1	0 ± 10	90 ± 5	0 ± 10
	23.4 ± 0.2	0.30 ± 0.05	−2465 ± 3	220 ± 20	−0.9 ± 0.1	0 ± 10	90 ± 5	0 ± 10
(CO)$_5$MnSnPh$_3$	18.6 ± 0.1	0.08 ± 0.02	−2535 ± 5	215 ± 10	−0.95 ± 0.05	40 ± 10	87 ± 1	0 ± 10
(CO)$_5$MnPbPh$_3$	11.9 ± 0.1	0.05 ± 0.05	−2395 ± 5	100 ± 10	−0.7 ± 0.1	0 ± 10	70 ± 5	0 ± 10
	12.0 ± 0.1	0.05 ± 0.05	−2390 ± 5	100 ± 10	−0.7 ± 0.1	0 ± 10	70 ± 5	0 ± 10
	10.7 ± 0.1	0.10 ± 0.05	−2381 ± 5	90 ± 10	−0.7 ± 0.1	0 ± 10	74 ± 5	0 ± 10
	10.5 ± 0.1	0.10 ± 0.05	−2376 ± 5	90 ± 10	−0.7 ± 0.1	0 ± 10	74 ± 5	0 ± 10

[a] The chemical shift parameters are defined as follows. $\delta_{33} \leq \delta_{22} \leq \delta_{11}$, $\delta_{iso} = (\delta_{11} + \delta_{22} + \delta_{33})/3$, $\Omega = \delta_{11} - \delta_{33}$, $\kappa = 3(\delta_{22} - \delta_{iso})/\Omega$.[66] The components of the chemical shift tensor are $\delta_{ii} = (\nu_{ii} - \nu_{ref})/\nu_{ref}$ (ii = 11, 22, 33). The EFG parameters are $C_Q = eQV_{ZZ}/h$ and $\eta_Q = (V_{XX} - V_{YY})/V_{ZZ}$ where $|V_{ZZ}| \geq |V_{YY}| \geq |V_{XX}|$, e is the electron charge, and h is Planck's constant. α, β and γ are the Euler angles that describe the relative orientation of the chemical shift tensor with respect to the EFG tensor.[67]

were employed. The default accuracy of the integration grid was modified to better describe the core orbitals, increasing *accint* to 5 and *accsph* to 6. Magnetic shielding values were referenced to the calculated isotropic shielding value of an isolated tetrahedral MnO_4^- ion (Mn−O bond length = 1.602 Å), $\delta = (\sigma_{ref} - \sigma_{sample})/(1 - \sigma_{ref})$. Recent computation studies by Bühl indicate that the manganese shielding of an isolated permanganate ion (equilibrium structure) becomes deshielded by 35 ppm on dissolution in water.[46]

Results and Discussion

1. Analysis of ^{55}Mn NMR Spectra. The ^{55}Mn NMR parameters obtained from the best-fit simulations of the NMR spectra acquired for η^5-CpMn(CO)$_3$, Mn$_2$(CO)$_{10}$, and three group-14 substituted manganese pentacarbonyls are presented in Table 1. The C_Q values range from 3.28 MHz for Mn$_2$(CO)$_{10}$ to 64.3 MHz for η^5-CpMn(CO)$_3$. The spans, Ω, of the chemical shift tensors range from 105 to 920 ppm for Mn$_2$(CO)$_{10}$ and η^5-CpMn(CO)$_3$, respectively. Where possible, the EFG parameters available from early single-crystal ^{55}Mn NMR studies were used as a starting point for the spectral simulations.

1.1. η^5-CpMn(CO)$_3$. The ^{55}Mn NMR spectra (central transition) obtained of a powder sample of η^5-CpMn(CO)$_3$ are shown in Figure 1. The spectrum acquired at 21.14 T was collected with a single transmitter offset. The spectrum is ca. 700 kHz broad and is dominated by a quadrupolar coupling constant of 64.3 MHz. For comparison, the ^{55}Mn NMR spectra obtained at 7.05 and 11.75 T are also presented. The QCPMG spectrum at 7.05 T was acquired using 25 different, evenly spaced, steps of the transmitter while the QCPMG, and echo spectra acquired at 11.75 T were collected in 12 and 6 steps, respectively.[32] The spectrum acquired at 21.14 T shows all the features necessary to accurately determine both the ^{55}Mn EFG and chemical shift parameters.

When both an EFG and anisotropic chemical shift are present, the line shape of the central transition spectrum of a half-integer quadrupolar nucleus can be used to obtain information about the EFG and chemical shift tensors. If a rotation axis (C_n, $n \geq 3$) passes through the nucleus of interest, the EFG and chemical shift tensors must be axially symmetric. In the case of η^5-CpMn(CO)$_3$, X-ray diffraction

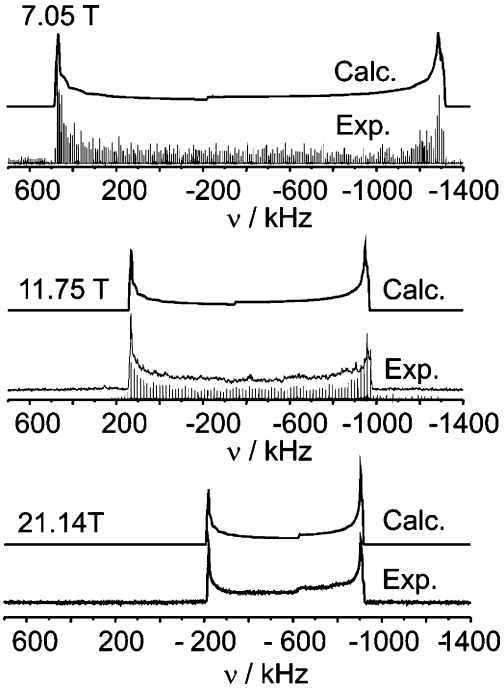

Figure 1. Central transition ^{55}Mn NMR spectra of stationary samples of η^5-CpMn(CO)$_3$ acquired at 7.05, 11.75, and 21.14 T. Spectra simulated using the parameters contained in Table 1 are presented above experimental spectra. The spectra acquired at 7.05 and 11.75 T were acquired using several different transmitter offsets, while the spectrum at 21.14 T was collected with a single transmitter offset.

indicates the molecule possesses C_1 symmetry;[47] however, the deviations from D_{5h} and C_{3v} symmetries in the Cp ring and the Mn(CO)$_3$ fragments, respectively, are negligible.[48] Furthermore, the Cp ring is thought to have a low barrier to internal rotation. From consideration of this information together with the NMR data, it is clear that the EFG tensor is axially symmetric with the unique component, V_{ZZ}, along the approximate C_3 axis, Figure 2. This leaves two possible orientations for the ^{55}Mn chemical shift tensor; either the skew, $\kappa = 1$ and δ_{33} is parallel to V_{ZZ}, Figure 2e, or $\kappa = -1$ and δ_{11} is parallel to V_{ZZ}, Figure 2f. Clearly, the experimental spectrum obtained at 21.14 T is only consistent with the first possibility.

(44) Perdew, J. P. *Phys. Rev. B* **1986**, *33*, 8822−8824.
(45) Perdew, J. P. *Phys. Rev. B* **1986**, *34*, 7406.
(46) Bühl M. *J. Phys. Chem. A* **2002**, *106*, 10505−10509.
(47) Fitzpatrick, P. J.; Le Page, Y.; Sedman, J.; Butler, I. S. *Inorg Chem.* **1981**, *20*, 2852−2861.
(48) Full, J.; González, L.; Daniel, C. *J. Phys. Chem. A* **2001**, *105*, 184−189.

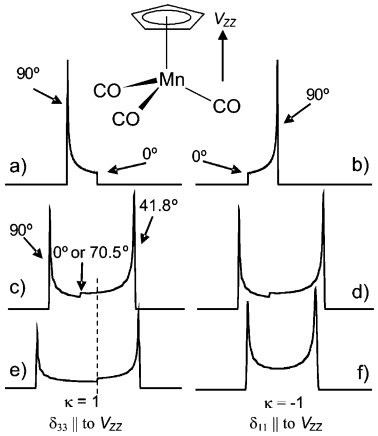

Figure 2. Calculated ^{55}Mn NMR spectra showing the interplay of the EFG and chemical shift parameters on the powder line shape. (a) $C_Q = 0$ MHz, $\kappa = 1$, $\Omega = 920$ ppm; (b) $C_Q = 0$ MHz, $\kappa = -1$, $\Omega = 920$ ppm; (c,d) $C_Q = 64.3$ MHz, $\Omega = 0$ ppm; (e) $C_Q = 64.3$ MHz, $\kappa = 1$, $\Omega = 920$ ppm; (f) $C_Q = 64.3$ MHz, $\kappa = -1$, $\Omega = 920$ ppm. For all simulations $\eta = 0$ and the unique components of the two tensors are coincident. The angles indicate the orientation of the unique component of the tensors with respect to B_0. The dashed line shows the effect that Ω has on the position of the shoulder in the center of the axially symmetric powder pattern.

The position of the small shoulder near the center of the axially symmetric pattern strongly depends on the magnitude of the chemical shift anisotropy; this is indicated by the dashed line in Figure 2c and e for $\Omega = 0$ and 920 ppm, respectively. The shoulder is not observable in the spectra acquired at lower fields due to the stepwise acquisition method used and lower signal-to-noise. For many quadrupolar nuclei, large nuclear quadrupolar couplings typically limit solid-state NMR investigations. The ability to acquire NMR spectra of spin-5/2 nuclei with C_Q values in excess of 50 MHz in a straightforward, single offset experiment opens the door to characterizing EFG tensors in molecules with ^{55}Mn and other noninteger spin transition metal nuclei with moderate quadruple moments.

The values of C_Q and η_Q obtained from simulation of the powder line shapes, Table 1, are in agreement with an earlier single-crystal ^{55}Mn NMR study of Spiess and Sheline which found C_Q and η_Q to be 64.275 MHz and 0.0134, respectively.[23] The Ω and κ of the chemical shift tensor are determined to be 920 ppm and 0.95, respectively. As already indicated, the orientation of the two tensors is such that V_{ZZ} and the unique component of the chemical shift tensor, δ_{33}, are along the pseudorotation axis of the molecule, Figure 2. Large spans have been previously reported for other "piano stool" compounds. For example, the molybdenum chemical shift anisotropy for mesitylenetricarbonylmolybdenum is 775 ppm with $\kappa = 0.87$.[2] The origin of the large metal shielding anisotropy in transition metal "piano stool" compounds lies in the availability of symmetry appropriate virtual d orbitals.[49,50]

The paramagnetic contribution to shielding, which is normally negative, is related to the magnetic-dipole-allowed mixing between symmetry appropriate occupied and virtual molecular orbitals, MOs.[51,52] Qualitatively, the magnitude of the paramagnetic term is dependent both on the energy difference between the two orbitals and the matrix elements of the form $\langle\varphi_{virt}|\hat{L}_i|\varphi_{occ}\rangle$, where φ_{virt} and φ_{occ} are the virtual and occupied orbital wave functions and $\hat{L}_i$ is the angular momentum operator acting along i.[51,52] On the basis of the simple MO model proposed by Lichtenberger and Fenske for η^5-CpMn(CO)$_3$, the highest occupied molecular orbitals are localized on the metal and, to a good approximation, may be described as d_{z^2}, $d_{x^2-y^2}$, and d_{xy} orbitals, as illustrated in Figure 3 (the molecule is oriented such that the pseudorotation axis is along the z axis).[49] The lowest-lying virtual orbitals are of d_{xz} and d_{yz} character.[48,53] The assumption that the Mn MOs in η^5-CpMn(CO)$_3$ can be described by the atomic d orbitals is clearly an approximation; nevertheless, the symmetry of the metal d orbitals provides a qualitative understanding of the manganese shielding tensor. The matrix in Figure 3 shows the result of using the angular momentum operators (left column) on the occupied MOs (top row). By applying the magnetic field in the xy plane, mixing can occur between the occupied MOs and the virtual MOs; for example, applying $\hat{L}_y$ to $\varphi_{occ} = d_{xy}$ generates a d_{xz} orbital which can mix with $\varphi_{virt} = d_{xz}$.[52] Since there is a relatively small energy gap between these orbitals, the paramagnetic term will be substantial,[48] and the result will be an overall deshielding of the Mn nucleus in the xy plane, i.e., σ_{11} and σ_{22}. When the magnetic field is applied along the z direction, $\hat{L}_z$ operating on the three highest occupied orbitals does not result in efficient mixing with either φ_{virt}, and therefore, the paramagnetic contribution along z, i.e., σ_{33}, is small.[2,52]

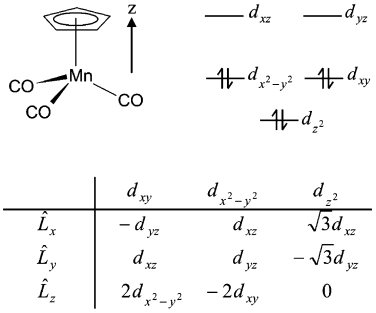

	d_{xy}	$d_{x^2-y^2}$	d_{z^2}
$\hat{L}_x$	$-d_{yz}$	d_{xz}	$\sqrt{3}d_{xz}$
$\hat{L}_y$	d_{xz}	d_{yz}	$-\sqrt{3}d_{yz}$
$\hat{L}_z$	$2d_{x^2-y^2}$	$-2d_{xy}$	0

Figure 3. The simplified orbital diagram for η^5-CpMn(CO)$_3$. The orbitals are derived from the Mn(CO)$_3^+$ fragment as taken from ref 49. Below is a section taken from Table 3 in ref 52 which indicates the effects that the angular momentum operators, first column, have on the occupied orbitals, first row.

The ^{55}Mn C_Q value in η^5-CpMn(CO)$_3$ is much larger than the ^{95}Mo C_Q in mesitylenetricarbonylmolybdenum, 0.96 MHz, despite their similar structures. Simply scaling the ^{95}Mo C_Q by the ratio of $Q(^{55}\text{Mn})/Q(^{95}\text{Mo})$, a ^{55}Mn C_Q of 14.4 MHz would be expected, significantly smaller than that observed for η^5-CpMn(CO)$_3$. The small ^{95}Mo C_Q value for mesitylenetricarbonylmolybdenum was rationalized on the basis of the geometry of the molecule, in particular implying that

(49) Lichtenberger, D. L.; Fenske, R. F. *J. Am. Chem. Soc.* **1976**, *98*, 50−63.
(50) Albright, T. A. *Acc. Chem. Res.* **1982**, *15*, 149−55.
(51) Ramsey, N. F. *Phys. Rev.* **1950**, *78*, 699−703.
(52) Jameson, C. J.; Gutowsky, H. A. *J. Chem. Phys.* **1964**, *40*, 1714−1724.
(53) Daniel, C.; Full, J.; González, L.; Kaposta, C.; Krenz, M.; Lupulescu, C.; Manz, J.; Minemoto, S.; Oppel, M.; Rosendo-Francisco, P.; Vajda, Š.; Wöste, L. *Chem. Phys.* **2001**, *267*, 247−260.

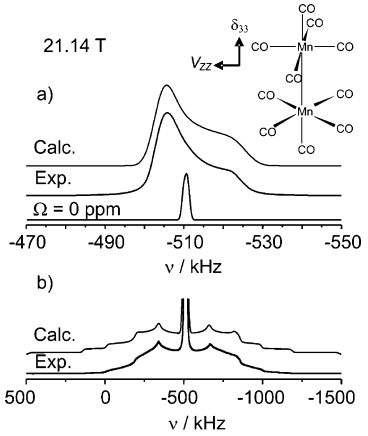

Figure 4. ^{55}Mn NMR spectra of a stationary sample of $Mn_2(CO)_{10}$ acquired at 21.14 T. (a) Central transition and (b) entire ^{55}Mn NMR spectrum including central and satellite transitions. The central transition spectrum is dominated by the chemical shift anisotropy at the ultrahigh field. Upper spectra were simulated using the parameters listed in Table 1, while the bottom spectrum in (a) is the calculated spectrum without including ^{55}Mn chemical shift anisotropy (i.e., $\Omega = 0$ ppm). The inset shows the structure of $Mn_2(CO)_{10}$ and the orientation of the unique components of the ^{55}Mn EFG and chemical shift tensors.

since the angles between the Mo−CO bond and the pseudorotation axis ($\theta = 53.9°$, 52.8°, and 54.3°) were close to the magic angle, 54.7356°, a small EFG would be expected.[2,54] For η^5-CpMn(CO)$_3$, θ is also close to the magic angle, 56.1°, 56.0°, and 56.3°, and yet a large C_Q is observed. Clearly factors other than θ must be responsible for the significant EFG at Mn.

We have used the atomic coordinates available from X-ray crystallography to perform quantum chemical calculations of the Mn shielding and EFG tensors.[47] The results presented in Table 1 are in good agreement with experiment given that some differences may result from the calculation being performed on an isolated molecule.[55] The agreement with experiment is a strong indicator that in the case of η^5-CpMn(CO)$_3$ both the EFG at Mn and the chemical shift parameters are predominantly determined by the local molecular structure.

1.2. $Mn_2(CO)_{10}$. The ^{55}Mn NMR spectrum of the central transition, $m_I = 1/2 \leftrightarrow m_I = -1/2$, of a stationary sample of $Mn_2(CO)_{10}$ acquired at 21.14 T is completely dominated by anisotropic shielding, Figure 4a. The single-crystal X-ray diffraction structure of $Mn_2(CO)_{10}$ reveals that there is a C_2 axis through the midpoint of the Mn−Mn bond, resulting in only one unique manganese site.[56] When simulating the ^{55}Mn NMR spectra acquired at 11.75 T (not shown), a homonuclear dipolar coupling of 305 Hz was required; the dipolar coupling did not significantly influence the spectrum acquired at 21.14 T.[57] The dipolar coupling of 305 Hz corresponds

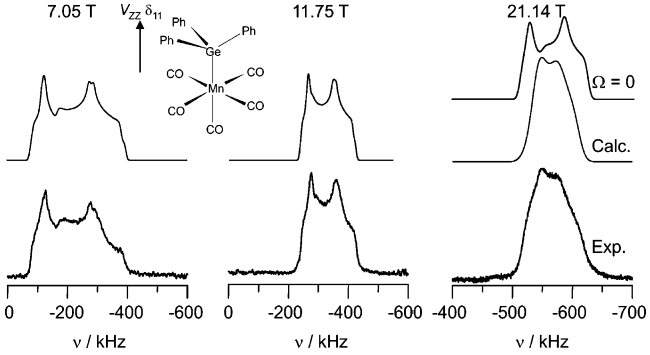

Figure 5. ^{55}Mn NMR spectra of stationary samples of $(CO)_5MnGePh_3$ acquired at 7.05, 11.75, and 21.14 T. Spectra simulated using the parameters contained in Table 1 are presented above experimental spectra. The top spectrum at 21.14 T is the calculated spectrum without including chemical shift anisotropy (i.e., $\Omega = 0$ ppm). The inset shows the structure of $(CO)_5MnGePh_3$ and the orientation of the unique components of the ^{55}Mn EFG and chemical shift tensors.

well to the value calculated on the basis of the Mn−Mn bond length, 2.9042 Å, determined from X-ray diffraction.[56] The simulations also included the effects of $^1J(^{55}Mn,^{55}Mn)$ which has been reported as 65 Hz; this coupling constant had a negligible effect on the calculated spectra.[58] Figure 4b shows the entire ^{55}Mn NMR spectrum (central and satellite transitions) of a stationary sample of $Mn_2(CO)_{10}$. The spectrum is approximately 2.0 MHz broad and therefore could not be completely excited using a single transmitter offset. Despite the distortions, the discontinuities were found to be sensitive to both the EFG and chemical shift parameters. The C_Q and η_Q values determined are consistent with previous measurements.[18,20,58]

The manganese chemical shift tensor has not been previously characterized for $Mn_2(CO)_{10}$. Due to the presence of the quadrupolar, dipolar, and indirect spin−spin coupling, accurately determining the chemical shift tensor at lower applied magnetic field strengths is difficult; for example, the spectrum acquired at 7.05 T for a stationary sample is a relatively featureless peak.[59] The V_{ZZ} component of the EFG tensor is oriented 90° from the Mn−Mn dipolar vector, in agreement with the early single-crystal ^{55}Mn NMR study.[20] On the basis of the Euler angles that describe the relative orientation of the EFG and chemical shift tensors, the unique component of the chemical shift tensor is along the Mn−Mn bond, Figure 4. The orientations of the tensors are discussed further in a later section.

1.3. $(CO)_5MnGePh_3$. The crystal structure of $(CO)_5MnGePh_3$ has not been reported, but previous single-crystal ^{55}Mn NMR studies indicate that there are two crystallographically unique Mn sites.[24] The presence of two sites was confirmed by MAS measurements (spinning rate, 35 kHz) at 21.14 T. The ^{55}Mn NMR spectra of stationary samples acquired at the three fields are presented in Figure 5. The spectra acquired at 7.05 and 11.75 T could be fit without including chemical shift anisotropy. The quadrupolar coupling parameters determined from the stationary sample spectra, Table 1, are in good

(54) Akitt, J. W.; McDonald, W. S. *J. Magn. Reson.* **1984**, *58*, 401−412.
(55) Ooms, K. J.; Feindel, K. W.; Willans, M. J.; Wasylishen, R. E.; Hanna, J. V.; Pike, K. J.; Smith, M. E. *Solid State Nucl. Magn. Reson.* **2005**, *28*, 125−134.
(56) Churchill, M. R.; Amoh, K. N.; Wasserman, H. J. *Inorg. Chem.* **1981**, *20*, 1609−1611.
(57) The simulation program does not properly treat the residual dipolar coupling to the neighboring quadrupolar nucleus which arises from the second-order quadrupolar perturbation on the neighboring Mn. Given that the C_Q is small, this is not likely to significantly affect the simulated line shapes.
(58) Wi, S.; Frydman, L. *J. Chem. Phys.* **2000**, *112*, 3248−3261.
(59) Siegel, R.; Nakashima, T. T.; Wasylishen, R. E. *Chem. Phys. Lett.* **2006**, *421*, 529−533.

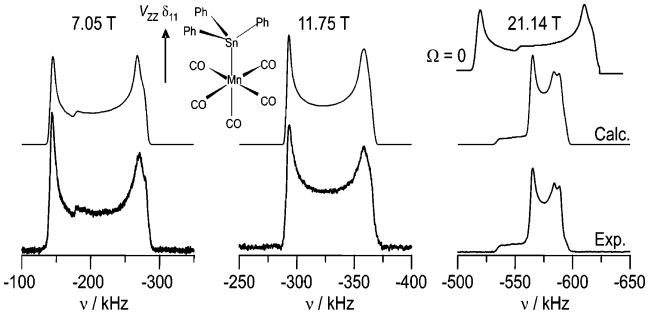

Figure 6. ^{55}Mn NMR spectra of stationary samples of $(CO)_5MnSnPh_3$ acquired at 7.05, 11.75, and 21.14 T. Spectra simulated using the parameters contained in Table 1 are presented above experimental spectra. The top spectrum at 21.14 T is the calculated spectrum without including chemical shift anisotropy (i.e., $\Omega = 0$ ppm). The inset shows the structure of $(CO)_5MnSnPh_3$ and the orientation of the unique components of the ^{55}Mn EFG and chemical shift tensors.

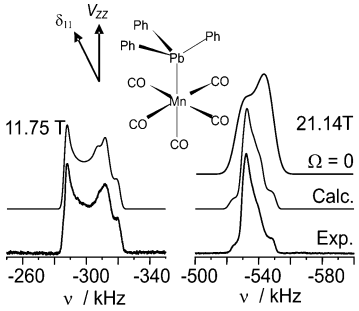

Figure 7. ^{55}Mn NMR spectra of stationary samples of $(CO)_5MnPbPh_3$ acquired at 11.75 and 21.14 T. Spectra simulated using the parameters contained in Table 1 are presented above experimental spectra. The top spectrum at 21.14 T is the calculated spectrum without including chemical shift anisotropy (i.e., $\Omega = 0$ ppm). The inset shows the structure of $(CO)_5MnPbPh_3$ and the orientation of V_{ZZ} and δ_{11}.

agreement with the previous single-crystal ^{55}Mn NMR results.[24] The spectrum of a stationary sample acquired at 21.14 T requires the inclusion of chemical shift anisotropy and reveals $\Omega = 220$ ppm and $\kappa = -0.95 \pm 0.05$.

1.4. $(CO)_5MnSnPh_3$. The ^{55}Mn NMR line shapes of stationary samples of $(CO)_5MnSnPh_3$ show dramatic differences at the different applied magnetic field strengths, Figure 6. The crystal structure determined by X-ray diffraction indicates that there are four unique molecules in the unit cell; however, it is not clear which solvent was used for the crystallization.[60] The ^{55}Mn NMR spectra of stationary samples, shown in Figure 6, and of an MAS sample spinning at 30 kHz, not shown, and previous single-crystal ^{55}Mn NMR results all indicate that there is only one Mn site;[24] hexane was used to recrystallize $(CO)_5MnSnPh_3$ in this study. This indicates that there are different polymorphs of $(CO)_5MnSnPh_3$; polymorphism has previously been noted for $(CO)_5MnPbPh_3$.[61] The quadrupolar parameters determined here, Table 1, are in good agreement with the previous single-crystal ^{55}Mn NMR study.[24] Accurately characterizing the chemical shift tensor is difficult based on the spectra acquired at 7.05 and 11.75 T; however, at 21.14 T, the experimental NMR spectrum cannot be fit without including a Ω of 215 ppm.

1.5. $(CO)_5MnPbPh_3$. The crystal structure of $(CO)_5MnPbPh_3$ is unknown; therefore, any insight regarding the structure of $(CO)_5MnPbPh_3$ is valuable. The breadth of the ^{55}Mn NMR spectra of stationary samples of $(CO)_5MnPbPh_3$, Figure 7, reveal that the ^{55}Mn C_Q values are smaller than for either the analogous Sn or Ge compounds. The ^{55}Mn NMR spectrum of the MAS sample could not be fit with the two sites determined in an earlier single-crystal NMR study.[24] To determine the C_Q parameters more accurately, a 3Q-MAS spectrum was acquired at 21.14 T, Figure 8. The high applied magnetic field strength enabled four sites with slightly different values for δ_{iso}, C_Q, and η_Q to be distinguished, Table 1. Acquisition of this spectrum would be difficult at lower applied magnetic field strengths, as the large quadrupolar broadening would require much higher spinning rates and

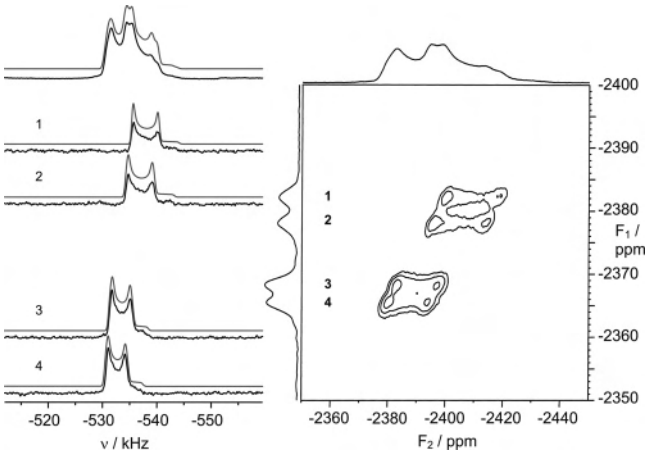

Figure 8. ^{55}Mn NMR 3Q MAS spectra of $(CO)_5MnPbPh_3$ acquired at 21.14 T, with $\nu_{rot} = 15$ kHz. On the left are the four anisotropic slices taken through the four sites; simulated spectra are presented above experimental spectra. The top spectrum on the left is the spectrum collected under MAS conditions at 21.14 T.

the four sites may not be adequately resolved. The presence of four sites indicates that a different polymorph of $(CO)_5MnPbPh_3$ is obtained when recrystallized from hexane than was previously obtained from methanol. In general, when performing transition metal SSNMR on powder samples, the presence of multiple crystallographic sites can make accurate determination of the NMR parameters from one-dimensional spectra difficult or impossible; however, the MQMAS experiment allows for the separation of the different sites into a second dimension.[62] The ability to differentiate sites with small differences in δ_{iso} and C_Q at ultrahigh-field strengths, as demonstrated here, is an important step to applying SSNMR to the study of more complex transition metal complexes.

2. Electric Field Gradients at Mn in $(CO)_5MnY$ Compounds. On the basis of a point charge analysis of the EFG in octahedral transition metal compounds, MX_5Y compounds with ideal geometries, i.e., equal bond lengths and angles, should have a substantial, axially symmetric EFG at the metal center.[63] The magnitude of the EFG at M depends on differences in the electronic properties of X and Y.

(60) Weber, H. P.; Bryan, R. F. *Acta Crystallogr.* **1967**, *22*, 822−836.
(61) Christendat, D.; Butler, I. S.; Gilson, F. R.; Morin, D. F. G. *Can. J. Chem.* **1999**, *77*, 1892−1898.
(62) Medek, A.; Harwood: J. S.; Frydman, L. *J. Am. Chem. Soc.* **1995**, *117*, 12779−12787.
(63) Han, O. H.; Oldfield, E. *Inorg. Chem.* **1990**, *29*, 3666−3669.

Table 2. Principal Components of the ^{55}Mn Chemical Shift Tensors for the Compounds Studied

	δ_{11}/ppm	δ_{22}/ppm	δ_{33}/ppm	δ_{iso}	Ω/ppm
η^5-CpMn(CO)$_3$	-1885 ± 10	-1908 ± 10	-2805 ± 5	-2200 ± 10	920 ± 10
Mn$_2$(CO)$_{10}$	-2252 ± 5	-2255 ± 5	-2357 ± 5	-2288 ± 2	105 ± 10
(CO)$_5$MnGePh$_3$	-2325 ± 10	-2534 ± 10	-2545 ± 10	-2468 ± 3	220 ± 20
	-2322 ± 10	-2531 ± 10	-2542 ± 10	-2465 ± 3	220 ± 20
(CO)$_5$MnSnPh$_3$	-2393 ± 5	-2603 ± 10	-2608 ± 5	-2535 ± 5	215 ± 10
(CO)$_5$MnPbPh$_3$[a]	-2333 ± 5	-2418 ± 5	-2433 ± 5	-2395 ± 5	100 ± 10
	-2325 ± 5	-2402 ± 5	-2416 ± 5	-2381 ± 5	90 ± 10

[a] For (CO)$_5$MnPbPh$_3$, the differences in the Eulers angles, Ω, κ between sites 1 and 2, as well as 3 and 4, were not observable.

Deviations from ideal octahedral geometry, either in the local molecular structure or the long-range crystal packing, can also play a role in determining the magnitude and orientation of the principal components of the EFG in the molecular frame.

For Mn$_2$(CO)$_{10}$, the ^{55}Mn C_Q is small compared to the known range of ^{55}Mn C_Q values and the orientation of the EFG tensor is surprising (i.e., V_{ZZ} is not along the Mn−Mn bond, Figure 4). The nuclear quadrupolar coupling constant,$C_Q = eQV_{ZZ}/h$, depends on the largest component of the EFG, V_{ZZ}, and the nuclear quadrupole moment, Q. Since Q is relatively large for ^{55}Mn, a C_Q of 3.28 MHz translates into a very small V_{ZZ}; the charge distribution about the Mn is nearly spherical, an unusual case for an MX_5Y complex. The orientation of the EFG tensor suggests that distortion in the octahedral geometry, i.e., different ligand bond lengths and bond angles and lattice effects, are likely responsible for the EFG at the Mn nucleus rather than the MX_5Y coordination. The dominant role of small structural distortions to the EFG is also emphasized by the value of η_Q, 0.35. If an isolated Mn$_2$(CO)$_{10}$ molecule had a C_4 symmetry axis passing through the Mn site, the η_Q would be 0, but the distortions in the structure,[56] such as the fact that the OC−Mn−Mn bond angle is not 180°, break the C_4 symmetry and result in the nonzero value of η_Q.

The ^{55}Mn C_Q values of (CO)$_5$MnMPh$_3$ (M = Ge, Sn, Pb) are an order of magnitude larger than for Mn$_2$(CO)$_{10}$ and decrease as M becomes heavier, in agreement with previous results.[24] As has been previously noted, this conforms to the trend in the electronegativities of the M atoms, $\chi_{Ge} = 2.02$, $\chi_{Sn} = 1.72$, $\chi_{Pb} = 1.55$.[64] The larger C_Q values suggest that the EFG is likely dominated by the MX_5Y coordination geometry and that the distortions from octahedral geometry introduced by the lattice will be a secondary contribution. The orientation of the EFG tensor is expected to be such that V_{ZZ} is nearly parallel to the Mn−M bond.[24] The MPh$_3$ groups destroy the C_4 local symmetry at Mn, and consequently, there are no symmetry-related reasons for the ^{55}Mn EFG or chemical shift tensors to be axially symmetric.

The four unique sites resolved in (CO)$_5$MnPbPh$_3$ demonstrate that, even when the EFG is dominated by the charge distribution created by the MX_5Y geometry, changes in the EFG due to subtle variations in molecular structure can be detected. Despite being the same molecules, the ^{55}Mn C_Q values of the four sites vary by up to 15%.

For (CO)$_5$MnSnPh$_3$ and (CO)$_5$MnPbPh$_3$, the EFG tensors are nearly axially symmetric, $\eta_Q \leq 0.10$. The EFG tensor at the Mn in (CO)$_5$MnSnPh$_3$ and (CO)$_5$MnPbPh$_3$ is dictated primarily by the approximate C_4 local symmetry and is relatively unaffected by the three phenyl rings which break the rotational symmetry. For (CO)$_5$MnGePh$_3$ the η_Q values for the two sites are 0.30 and 0.36, indicating that eQV_{XX}/h and eQV_{YY}/h differ by 8.8 and 5.8 MHz; these differences are more than twice the C_Q value of Mn$_2$(CO)$_{10}$.

The ability to observe small variations in the EFG of MX_5Y complexes is an important step toward using SSNMR to characterize transition metal solids. Structural distortions are routinely investigated using SSNMR of MX_6 and *fac*-MX_3Y_3 complexes because these complexes typically yield small or zero EFGs.[63] The ability to perform NMR of solids with large C_Q values will lead to greater sensitivity in detecting different contributions to the EFG tensor, e.g., ligand charge distribution versus distortions in geometry.

3. Manganese Chemical Shift Anisotropies in (CO)$_5$MnY Compounds. The ^{55}Mn chemical shift tensors for the (CO)$_5$MnMPh$_3$ (M = Ge, Sn, Pb) complexes and Mn$_2$(CO)$_{10}$ do not display an obvious trend in any of the components of the chemical shift tensor as the M atom is changed, Table 2. The relative orientations of the chemical shift and EFG tensors can usually be obtained from analysis of an NMR powder pattern. If the orientation of the EFG tensor in the molecular frame is available from single-crystal NMR experiments, symmetry arguments, or computational quantum chemistry, then the orientation of the chemical shift tensor in the molecular frame can be obtained. As discussed previously, the unique component of the chemical shift tensor in the molecular frame for Mn$_2$(CO)$_{10}$, δ_{33}, is along the Mn−Mn bond, 90° from V_{ZZ}. Like Mn$_2$(CO)$_{10}$, (CO)$_5$MnGePh$_3$ and (CO)$_5$MnSnPh$_3$ have nearly axially symmetric chemical shift tensors. In both cases, the unique component of the chemical shift tensor, δ_{11}, is parallel to V_{ZZ} and is therefore along the M−M bond, Figures 5 and 6. In general, for MX_5Y complexes with ideal geometry, the unique component of the chemical shift tensor is expected to be along the Mn−Y bond. The chemical shift tensors for the four sites of (CO)$_5$MnPbPh$_3$ deviate from axial symmetry, $\kappa = 0.7$, and do not appear to be coincident with the EFG tensor.

The component of the chemical shift tensor approximately along the Mn−M bond arises from magnetic-dipole-allowed mixing of occupied and virtual molecular orbitals in a plane perpendicular to the Mn−M bond. Therefore, the shielding along the bond should be constant if there is no change in

(64) Alred, A. L.; Rochow, E. G. *J. Inorg. Nucl. Chem.* **1958**, *5*, 264−268.

the $Mn(CO)_4$ plane.[65] This appears to be true for $(CO)_5MnGePh_3$ and $(CO)_5MnPbPh_3$, δ_{11} is approximately −2330 ppm, but δ_{11} for $(CO)_5MnSnPh_3$ is different. Density functional theory calculations on idealized structures did not reveal any obvious reasons for the different chemical shift parameters. Without crystal structures, further interpretation is impractical.

Conclusions

We have demonstrated some of the advantages of performing solid-state ^{55}Mn NMR spectroscopy at 21.14 T. The ability to extract small chemical shift anisotropies from NMR spectra that are dominated by the quadrupolar interaction at lower fields is established by studying $Mn_2(CO)_{10}$ and $(CO)_5MnMPh_3$ (M = Ge, Sn, Pb). The high resolution attainable at ultrahigh fields makes it possible to distinguish crystallographically nonequivalent sites in solid powder samples using MQMAS, even when the C_Q values are relatively large and the differences in isotropic chemical shifts are small. On the basis of small differences in the EFG tensors, information about distortions in the MX_5Y geometry can be obtained. In addition, SSNMR studies at ultrahigh fields offer the ability to perform routine, single-step acquisitions of samples where the C_Q is in excess of 60 MHz for spin $I \geq 5/2$ nuclei, as shown for η^5-$CpMn(CO)_3$. Clearly, the availability of ultrahigh-field magnets will facilitate NMR investigation of many other transition metal nuclei in solid inorganic and organometallic compounds.

Acknowledgment. The research was funded by the Natural Sciences and Engineering Research Council (NSERC) of Canada, the Canada Foundation for Innovation (CFI), the Alberta Ingenuity Fund, and the University of Alberta. R.E.W. is a Canada Research Chair in Physical Chemistry at the University of Alberta. Access to the 900 MHz NMR spectrometer was provided by the National Ultrahigh-Field NMR Facility for Solids (Ottawa, Canada), a national research facility funded by CFI, the Ontario Innovation Trust, Recherche Québec, the National Research Council of Canada, and Bruker BioSpin and managed by the University of Ottawa (www.nmr900.ca).

IC0608445

(65) Ooms, K. J.; Wasylishen, R. E. *Can. J. Chem.* **2006**, *84*, 300−308.
(66) Mason, J. *Solid State Nucl. Magn. Reson.* **1993**, *2*, 285−288.
(67) Willans, M. J.; Feindel, K. W.; Ooms, K. J.; Wasylishen, R. E. *Chem. Eur. J.*, **2006**, *12*, 159−168.